

# *Formation of supramolecular gels from host-guest interactions between PEGylated chitosan and $\alpha$ -cyclodextrin*

Article

Published Version

Creative Commons: Attribution 4.0 (CC-BY)

Open Access

Vandera, K.-K. A., Pague, C., Omar, J., González-Gaitano, G., Ways, T. M. M., Khutoryanskiy, V. V. ORCID: <https://orcid.org/0000-0002-7221-2630> and Dreiss, C. A. (2023) Formation of supramolecular gels from host-guest interactions between PEGylated chitosan and  $\alpha$ -cyclodextrin. *Macromolecular Materials and Engineering*, 308 (6). 2200646. ISSN 1439-2054 doi: 10.1002/mame.202200646 Available at <https://centaur.reading.ac.uk/109740/>

It is advisable to refer to the publisher's version if you intend to cite from the work. See [Guidance on citing](#).

To link to this article DOI: <http://dx.doi.org/10.1002/mame.202200646>

Publisher: Wiley

All outputs in CentAUR are protected by Intellectual Property Rights law, including copyright law. Copyright and IPR is retained by the creators or other copyright holders. Terms and conditions for use of this material are defined in the [End User Agreement](#).

[www.reading.ac.uk/centaur](http://www.reading.ac.uk/centaur)

## **CentAUR**

Central Archive at the University of Reading

Reading's research outputs online

# Formation of Supramolecular Gels from Host–Guest Interactions between PEGylated Chitosan and $\alpha$ -Cyclodextrin

Kalliopi-Kelli A. Vandera, Charlotte Pague, Jasmin Omar, Gustavo González-Gaitano, Twana Mohammed M. Ways, Vitaliy V. Khutoryanskiy, and Cécile A. Dreiss\*


Chitosan-based hydrogels are prepared via the formation of polypseudorotaxanes (PPR), by selectively threading  $\alpha$ -cyclodextrin ( $\alpha$ -CD) macrocycles onto polymeric chains, which, through the formation of microcrystalline domains, act as junction points for the network. Specifically, host–guest inclusion complexes are formed between  $\alpha$ -CD and PEGylated chitosan (PEG-Ch), resulting in the formation of supramolecular gels. PEG-grafted chitosan is obtained with a reaction yield of 79.8%, a high degree of grafting (50.9% GW) and water solubility ( $\approx 16 \text{ mg mL}^{-1}$ ), as assessed by turbidimetry. A range of compositions for mixtures of PEG-Ch solutions (0.2–0.8% w/w) and  $\alpha$ -CD solutions (2–12% w/w, or 0.04–0.2% mol) are studied. Regardless of PEG content, gels are not formed at low  $\alpha$ -CD concentrations (<4%). Dynamic rheology measurements reveal stiff gels ( $G'$  above 15k) and a narrow linear viscoelastic region, reflecting their brittleness. The highest elastic modulus is obtained for a hydrogel composition of 0.4% PEG-Ch and 6%  $\alpha$ -CD. Steady-state measurements, cycling between low and high shear rates, confirm the thixotropic nature of the gels, demonstrating their capacity to fully recover their mechanical properties after being exposed to high stress, making them good candidates to use as in-situ gel-forming materials for drug delivery to topical or parenteral sites.

## 1. Introduction

Interest in hydrogels for biomedical applications has exploded over the last several decades, due to their attractive features that include structural and mechanical similarity with natural tissues, versatility in building blocks, architecture, and functionality—including the potential to respond to triggers—and their capacity to encapsulate and release active compounds in a controlled manner.<sup>[1]</sup> Hydrogels are typically formed by the cross-linking of hydrophilic polymers, either chemically (through covalent bonds), or physically, through noncovalent approaches, including for instance hydrogen bonds, electrostatic interactions, or host–guest complexation.<sup>[2]</sup> In this work, we develop hydrogel formulations based on chitosan and poly(ethylene glycol) (PEG); both polymers have been widely investigated for biomedical applications, such as gene<sup>[3–5]</sup> and cell therapy,<sup>[6,7]</sup> wound dressing,<sup>[8,9]</sup> tissue regeneration,<sup>[9,10]</sup> and as delivery systems<sup>[11]</sup> for the controlled release of antibiotics<sup>[12,13]</sup> and macromolecules.<sup>[3]</sup>

K.-K. A. Vandera, C. Pague, J. Omar, C. A. Dreiss  
 Institute of Pharmaceutical Science  
 School of Cancer & Pharmaceutical Science  
 King's College London  
 Franklin-Wilkins Building  
 150 Stamford Street, London SE1 9NH, UK  
 E-mail: cecile.dreiss@kcl.ac.uk

G. González-Gaitano  
 Departamento de Química  
 Universidad de Navarra  
 Pamplona 31080, Spain  
 T. M. M. Ways  
 Department of Pharmaceutics  
 College of Pharmacy  
 University of Sulaimani  
 Sulaimani, Kurdistan Region 46001, Iraq  
 V. V. Khutoryanskiy  
 Reading School of Pharmacy  
 University of Reading  
 Whiteknights  
 Reading RG6 6AD, UK

 The ORCID identification number(s) for the author(s) of this article can be found under <https://doi.org/10.1002/mame.202200646>

© 2023 The Authors. Macromolecular Materials and Engineering published by Wiley-VCH GmbH. This is an open access article under the terms of the Creative Commons Attribution License, which permits use, distribution and reproduction in any medium, provided the original work is properly cited.

DOI: 10.1002/mame.202200646

The use of physical interactions to construct hydrogels is advantageous as it implies the presence of dynamic cross-links, which can be broken and reformed, either under the action of external stimuli (such as temperature, irradiation, or ultrasound) or shear (i.e., when going through a needle), making them attractive for drug delivery applications where the gel can be applied to a specific area by injection, reform in-situ and an active compound can be slowly released where desired.<sup>[1]</sup> Amongst the type of interactions used to build supramolecular gels, host–guest interactions, which rely on the inclusion of a molecule, a pendant group or a polymer chain within the cavity of a “host,” for instance, cyclodextrins are particularly attractive.<sup>[14,15]</sup> Cyclodextrins (CDs) are cyclic oligosaccharides containing ( $\alpha$ -1,4)-a-D-glucopyranose units obtained from the enzymatic degradation of starch.<sup>[16]</sup> They are toroidal molecules with a truncated cone structure having a relatively apolar inner cavity, lined with alkyl groups and glycosidic oxygen atoms, and a hydrophilic outer surface with hydroxyl groups on the rim of the molecules.<sup>[17]</sup> This peculiar structure explains their widespread use in pharmaceutical formulations for the purpose of encapsulating poorly water-soluble drugs, increasing their solubility, and therefore their bioavailability.<sup>[18,19]</sup> Supramolecular gels prepared using the complexation with cyclodextrins are broadly based on two approaches. The first relies on host–guest interactions between small guest molecules chemically grafted on a polymer chain and cyclodextrins (usually  $\beta$ -CD) attached to another chain, leading to the “zipping” of the two chains together due to their derivatization with complementary units.<sup>[11,20,21]</sup> This type of hydrogels has found applications as self-healing materials because they are injectable and can autonomously restore their initial properties in situ.<sup>[20,22,23]</sup> The second strategy relies on the formation of polypseudorotaxanes (PPR), also referred to as “molecular necklaces,” which are formed by the selective threading of CD rings on polymer chains, most often,  $\alpha$ -CD (6 glucopyranose units) on PEG chains.<sup>[24,25]</sup> The driving forces for the formation of PPRs include hydrophobic and van der Waals interactions between the cavity of  $\alpha$ -CD and the  $-\text{CH}_2\text{CH}_2\text{O}-$  units of PEG, as well as hydrogen bonding between the hydroxyl groups of adjacent  $\alpha$ -CD molecules threaded on the same polymer chain. In turn, hydrogen bonds formed between  $\alpha$ -CD molecules on neighbouring chains lead to the formation of microcrystalline regions, which act as cross-links for the network.<sup>[26–28]</sup> CDs with a larger cavity ( $\beta$ -CD and  $\gamma$ -CD) cannot establish strong interactions with PEG and thus hydrogel formation does not occur with this polymer.<sup>[24,25]</sup> Based on this concept, a range of supramolecular gels have been reported with polymers that include PEG in their motifs. For instance,  $\alpha$ -CD has been used to self-assemble PEO-PHB-PEO triblock copolymers, forming a thixotropic and injectable hydrogel for the sustained and controlled delivery of macromolecular drugs.<sup>[13]</sup> Multifunctional  $\alpha$ -CD-PEG hydrogels formed between PEG chains and  $\alpha$ -CD conjugated with genes, peptides, or other macromolecules have been explored for controlled cell delivery and gene therapy.<sup>[1,2]</sup> A thermoreversible gel based on a polysaccharide, comprising PEG-grafted-dextran with  $\alpha$ -CD, has been formed via supramolecular assembly and dissociation with a controllable transition temperature.<sup>[29]</sup> The same principle has also been utilized to incorporate PEG-modified nanoparticles into nanocomposite gels,<sup>[30]</sup> such as silver, silica, and gold nanoparticles.<sup>[11,12,27,31]</sup>

In this work, we apply this design principle to build an injectable material based on biocompatible components, by grafting PEG moieties on chitosan. Chitosan is a linear polysaccharide composed of randomly distributed  $\beta$ -linked D-glucosamine<sup>[1–4]</sup> and N-acetyl-D-glucosamine units. It is a relatively abundant, natural biopolymer, which has attracted wide interest for its wound-healing, adhesive, and antibacterial properties, as well as the accessibility of functional groups, well-suited for further chemical modifications.<sup>[10]</sup> Despite its attractive features as a biomedical material, chitosan’s poor solubility under physiological conditions (pH 6–8) limits its applicability, in addition to the need to introduce a cross-linking process to generate chitosan gels. An interesting approach to produce functional biomaterials is to introduce hydrophilic groups without modifying the initial chitosan skeleton, thus preserving the original properties.<sup>[32]</sup> PEG-modified chitosan enhances the solubility of this polysaccharide in water,<sup>[33]</sup> while at the same time giving access to the formation of chitosan-based hydrogels by further cross-linking the PEG chains.<sup>[9]</sup> PEG can be synthesized in various molecular weights and functionalized with different terminal end groups (aldehyde, carboxyl, carbonate, iodide, epoxy, acrylate, N-hydroxysuccinimide, maleimide, and sulfonate groups).<sup>[32]</sup> All these PEG derivatives are commonly used for the PEGylation of colloidal particles, proteins, and functional polymers.<sup>[34]</sup> The PEGylation of chitosan is usually achieved by the reaction between a methoxy-poly(ethylene glycol) (mPEG) derivative and the amine active group of chitosan.<sup>[35,36]</sup> PEGylated chitosan hydrogels combined with  $\text{TiO}_2$  nanoparticles have been explored, for instance, for cardiac tissue regeneration, and have shown enhanced cell retention activity and adhesion of cardiomyocytes.<sup>[7]</sup> Bioadhesive PEGylated chitosan hydrogels, modulated by enzymatic cross-linking, have also been proposed for wound-healing applications, and shown superior healing effects in a skin incision when compared with suture, fibrin glue, and cyanoacrylate.<sup>[9]</sup>

There is a clear interest in developing chitosan-based hydrogels that would preserve the attractive features of chitosan, while providing fast in-situ gelation after injection. The combination of PEGylated chitosan with  $\alpha$ -CD affords this possibility, imparting injectability, ease of preparation, while circumventing the need of chemical cross-linkers. There are, however, very few accounts of hydrogels based on this strategy. One recent example has reported injectable gels by mixing PEG with chitosan conjugated with  $\alpha$ -CD, for bone tissue engineering.<sup>[10]</sup> Huh et al. have also proposed a gel consisting of chitosan modified with 2 kDa monocarboxylated PEG, using carbodiimide as a coupling agent, and  $\alpha$ -CD.<sup>[37]</sup> X-ray diffraction measurements confirmed the presence of the channel-type crystalline structures typical of inclusion complexes (IC) with cyclodextrins, and the gels displayed thermoreversibility, due to the temperature-sensitive break-up of the host–guest junctions.

This work investigates the formation of a supramolecular hydrogel based on the spontaneous association of  $\alpha$ -CD with short PEG chains (5 kDa) grafted on chitosan. Oscillatory rheological measurements are employed to characterize the elastic properties of the gels as a function of composition and steady-state measurements to explore their capacity to recover after being submitted to high shear rates, and thus their suitability for injection.

**Table 1.** Characteristics of the synthesized PEG-chitosan.

Degree of PEGylation	Yield [%]	GW [%]	DS [%; $^1\text{H}$ NMR]
Low (LPEG-Ch)	80	28	11
High (HPEG-Ch)	83	51	16

## 2. Results and Discussion

### 2.1. Synthesis and Characterization of PEGylated Chitosan (PEG-Ch)

PEGylated chitosan with a high degree of grafting (51% GW) was synthesized with a reaction yield of 80%. Unmodified chitosan, PEG-COOH and PEG-Ch were characterized using proton NMR and FTIR to assess the reaction and determine the structure and degree of substitution (Table 1).

The  $^1\text{H}$  NMR spectrum of unmodified chitosan shows the presence of peaks at 3.06, 3.57–3.80, and 1.97 ppm corresponding to H2, H3–6, and  $\text{NHCOCH}_3$ , respectively (Figure 1). The NMR spectra of both types of PEG-chitosan showed a peak at 3.33 ppm due to the  $\text{OCH}_3$  group of  $\text{CH}_3\text{O-PEG-}$  and the intensity of this peak in HPEG-chitosan was higher than that of LPEG-chitosan. Peaks related to H3, H4, H5, and H6 overlapped with the peaks of  $\text{OCH}_2\text{CH}_2$  and  $\text{OCH}_2$  groups (b, c, and d) at (3.35–3.89 ppm) (Figure 1). The peaks of PEG-COOH and PEG-Ch were identified as highlighted in the literature.<sup>[38]</sup> The peak at 2.03–2.04 ppm in PEGylated chitosan belongs to methyl of residual acetate groups

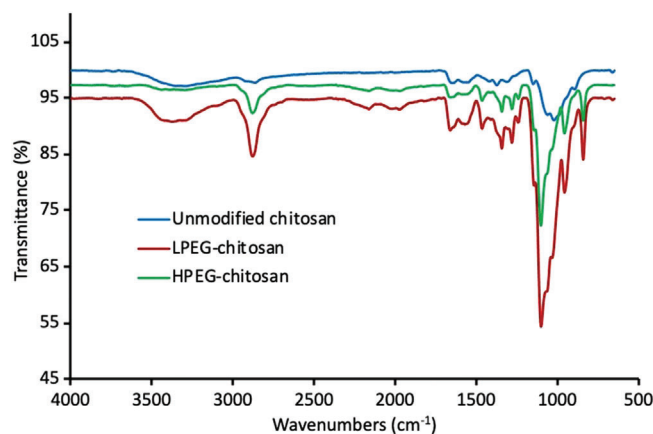


**Figure 2.** FTIR spectra of unmodified chitosan, LPEG-Ch, and HPEG-Ch.

and the peak at 1.88–1.90 ppm, present in both spectra of PEGylated chitosan, was reported previously but was not given any assignment.<sup>[39]</sup> It may be related to a residual isourea by-product of a coupling reaction involving EDC. Based on the  $^1\text{H}$  NMR analysis and Equation 3, a degree of substitution of 11% and 16% was established for LPEG-Ch and HPEG-Ch, respectively (Table 1).

The FTIR spectra of the unmodified chitosan and PEG-Ch are shown in Figure 2. The unmodified chitosan presents peaks at 3000–3600  $\text{cm}^{-1}$  generated by the stretching vibration of O–H and N–H bonds and at 1649  $\text{cm}^{-1}$  due to the amide group ( $\text{N-C=O}$ ) stretching. For both LPEG- and HPEG-chitosan, the

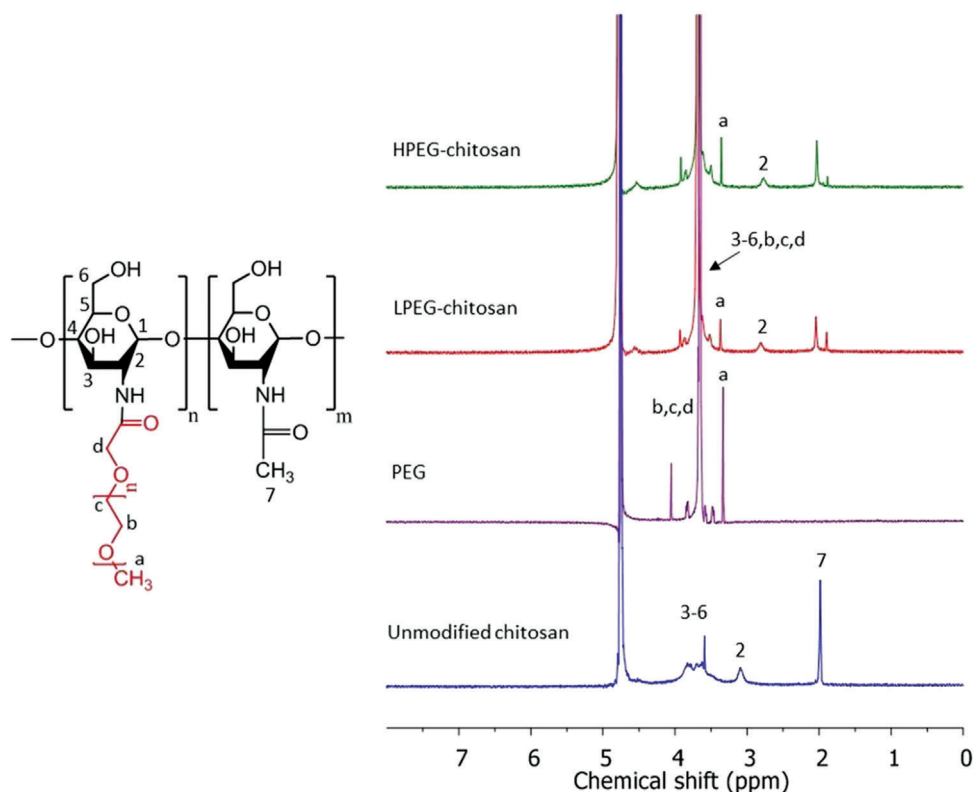


**Figure 1.**  $^1\text{H}$  NMR spectra of unmodified chitosan, PEG-COOH, LPEG-chitosan, and HPEG-chitosan.

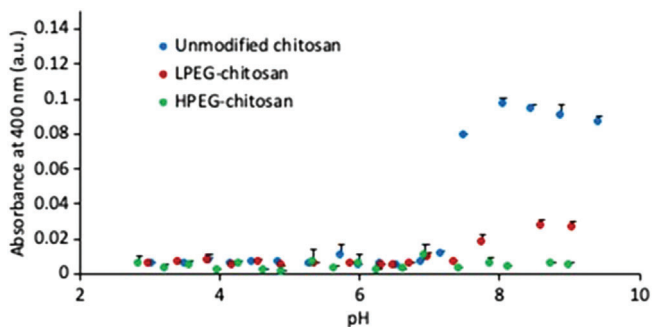


**Figure 3.** Effect of pH on the aqueous solubility of unmodified, LPEG-chitosan, and HPEG-chitosan.

characteristic peaks of PEG-Ch are observed at 841, 957, and 2878  $\text{cm}^{-1}$  and attributed to PEG groups. The peak at 1658  $\text{cm}^{-1}$  could correspond to the amide groups in the linker between PEG and chitosan. A weak ester peak at 1745  $\text{cm}^{-1}$  was also observed, as also reported elsewhere.<sup>[40]</sup> The intensity of these specific peaks in HPEG-chitosan was higher than LPEG-chitosan, indicating a higher degree of PEGylation of HPEG-chitosan than LPEG-chitosan.

## 2.2. Aqueous Solubility of PEG-Ch as a Function of pH (UV/Vis Spectroscopy)

The solubility of chitosan and PEG-grafted chitosan solutions was measured at a fixed concentration (0.05% w/w) and over a range of pH values. **Figure 3** shows that unmodified chitosan is soluble (illustrated by low turbidity or absorbance) at acidic pH, as expected due to the protonation of chitosan at low pH. However, it undergoes rapid precipitation (indicated by high turbidity or absorbance) at pH higher than 7.2. The solution of LPEG-chitosan is totally clear up to pH 7.4, but at pH 7.8, a very slight turbidity is observed (0.017 a.u.), which gradually increases by a further increase in the pH. Despite this, LPEG-chitosan shows a much higher solubility compared with unmodified chitosan. In contrast, HPEG-chitosan displays full aqueous solubility (illustrated by low turbidity) over the range of pH studied,<sup>[3–9]</sup> thus showing that a grafting of 50% PEG imparts solubility to the construct at pH values where chitosan is unprotonated.

Next, the solubility of HPEG-Ch in water (natural pH) was determined by measuring the turbidity using UV-Vis spectroscopy. In the absence of aggregates, scattering from the samples is nearly zero; the onset of aggregation is denoted by a break in the slope, with turbidity increasing linearly with concentration. **Figure 4** presents the changes of absorbance at 600 nm against PEG-Ch concentration, up to 2% w/w. The intersection of the two linear profiles is used as an estimation of the critical aggregation concentration (CAC) (1.6% w/w HPEG-Ch, equivalent to 0.8% PEG content). Previous studies have reported PEGylated chitosan (PEG 550–2000 Da) with DS of 16–20%, PEG content of 35–63%, and an aqueous solubility of 5  $\text{mg mL}^{-1}$  at pH below 8.<sup>[41,42]</sup> In another study, the solubility of chitosan (MW 10 kDa) was enhanced when conjugated with methoxy-PEG (2 kDa) (DS ranging from 5% to 19%), as reported from turbidimetry measurements.<sup>[33]</sup> Sugimoto et al. found that modified chitosan with high molecular-weight PEG (5 kDa), low DS

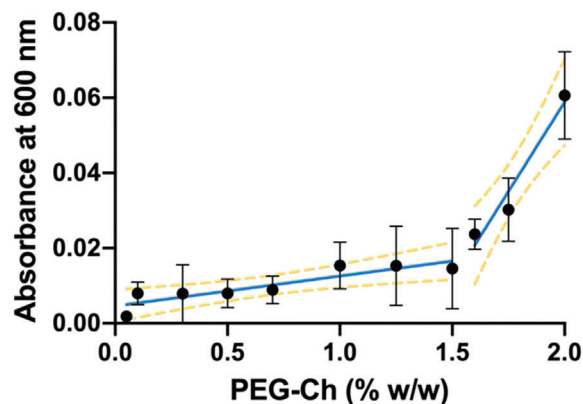


**Figure 4.** UV-Vis absorbance as a function of concentration of HPEG-Ch ( $n = 3$ ). The blue line is the linear regression fit and the yellow lines are the 95% confidence intervals. The intersection of the two linear models provides an estimate of the critical aggregation concentration.

(5–8%), and high GW (60–71%) was insoluble at pH 4–10.<sup>[41]</sup> Despite the high grafting densities, methoxy-PEG (MW 550 and 5000 Da) grafted on chitosan with molecular weight of 400 kDa could not dissolve in aqueous solution at pH 7, while PEG grafted on trimethyl chitosan produced clear solutions regardless of grafting density and PEG molecular weight.<sup>[43]</sup> Our HPEG-Ch shows remarkably high water solubility ( $\approx 16 \text{ mg mL}^{-1}$ ) compared with the reported values. This could be attributed to the molecular weight of PEG grafts (5000 Da) combined with the high DS of 16% and high GW of 50%. Tuning the degree of substitution (DS) and molecular weight of the grafted PEG (GW) leads to pH-independent solubility of PEGylated chitosan.<sup>[34]</sup>

## 2.3. Phase Diagram and Gel Formation

Given the much higher solubility of HPEG-Ch compared with LPEG-Ch, all studies presented in the rest of this work are performed on HPEG-Ch, which is therefore simply referred to as PEG-Ch.

Visual observation of a series of PEG-Ch and  $\alpha$ -CD mixtures in aqueous solution was used to build a phase diagram. The samples were classified according to their appearance as: liquid, weak gel, gel, and biphasic system (**Figure 5**). Gels, defined here as materials that did not flow when turned upside down after a few minutes of observation, were obtained for intermediate-to-high concentrations of grafted PEG and  $\alpha$ -CD, specifically ranging from 0.1% to 0.4% PEG (corresponding to PEG-Ch concentrations of 0.2–0.8%) and 6–12%  $\alpha$ -CD. Regardless of PEG content in the mixture, gels were not formed at low concentrations of  $\alpha$ -CD (2% and 4%), probably due to the resulting insufficient number of junctions for the network. At low PEG content (0.1%), either weak gels were obtained at intermediate  $\alpha$ -CD concentration (8%  $\alpha$ -CD), or biphasic systems with higher amounts of  $\alpha$ -CD (10% and 12%), presumably due to phase separation between a cross-linked PEG-rich phase and a water phase.

To confirm the nature of the gels, X-ray diffraction patterns were measured for two samples, comparing a mixture of PEG with  $\alpha$ -CD and the same PEG/ $\alpha$ -CD ratio for a mixture with PEG-Ch instead, for a composition in the gel phase area of the dia-



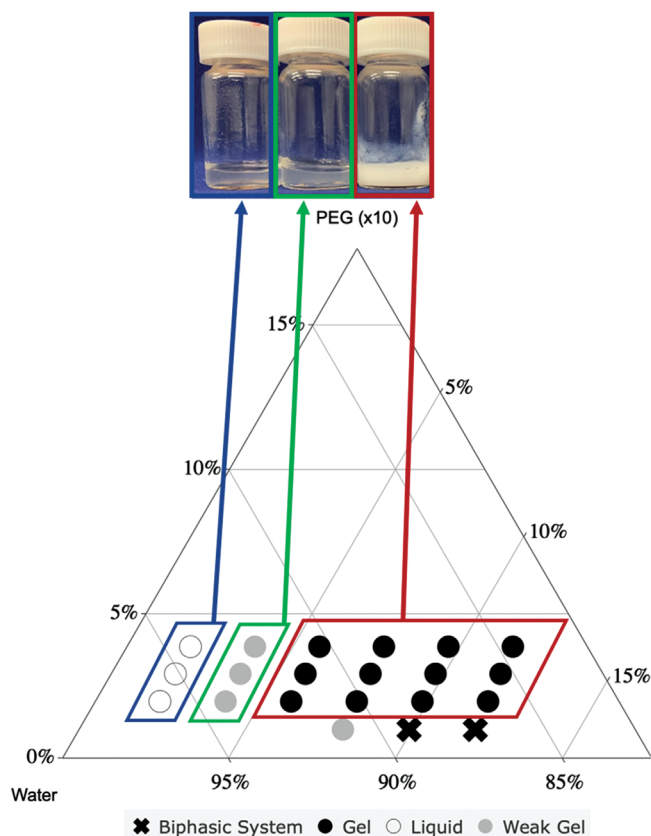


**Figure 5.** Phase diagram for mixtures of HPEG-Ch and  $\alpha$ -CD in aqueous solution: liquid (x), biphasic system (gray circles), weak gel (open circles), and gel (black circles) together with images showing the typical appearance of these samples for the corresponding states. The axis of the ternary plot represents the fraction of HPEG-Ch,  $\alpha$ -CD, and water in each sample. The concentration of grafted PEG in chitosan (0.1–0.4% w/w) corresponds to HPEG-Ch of 0.2–0.8% w/w. The PEG axis has been modified by multiplying the values by 10. The mole percentage range of  $\alpha$ -CD used was 0.004–0.2% that corresponds to the 2–12% w/w used in the diagram.

gram (Figure 6). In CD-PEG polypseudorotaxanes, the arrangement of macrocycles along the polymer axis and further packing produces channel-like structures with distinctive reflections in the XRD patterns, markedly different from the crystalline cage-type structure of the CD. The most intense peaks are at  $2\theta = 20.0^\circ$  ( $d = 4.44 \text{ \AA}$ ) and  $22.6^\circ$  ( $d = 3.96 \text{ \AA}$ ), assigned to the 210 and 300 reflections from the hexagonal lattice with  $a = 13.6 \text{ \AA}$ , and are the fingerprint of the CD channels.<sup>[44]</sup> In this case, the similar diffraction patterns obtained for both samples (Figure 6) confirm the presence of the channel-type crystalline structures in the PEG-Ch gels, which, acting as cross-links between the polymer chains, explain the formation of the gels.

#### 2.4. Rheology: Oscillatory Measurements

PEG-Ch/ $\alpha$ -CD mixtures that were visually observed to form self-sustaining gels (phase diagram, Figure 5) were assessed for their rheological properties. The linear viscoelastic region (LVR) was first evaluated by performing strain amplitude sweeps. Representative curves for gels comprising 0.3% grafted PEG and 6–

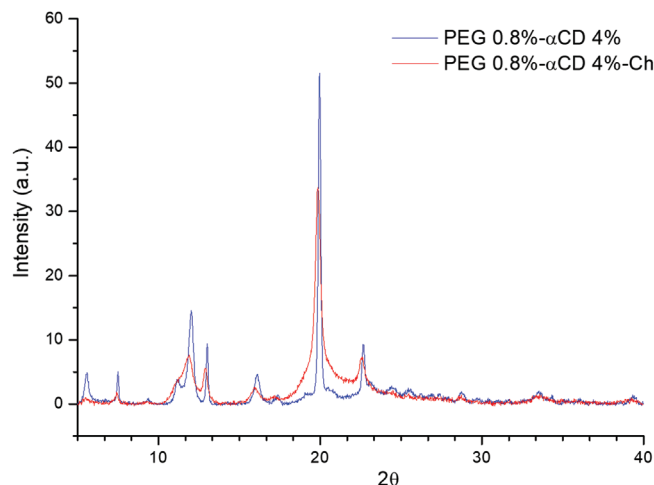


**Figure 6.** X-ray diffraction patterns comparing a mixture of 0.8% PEG with 4%  $\alpha$ -CD and the same PEG/ $\alpha$ -CD ratio for a PEG-Ch gel.

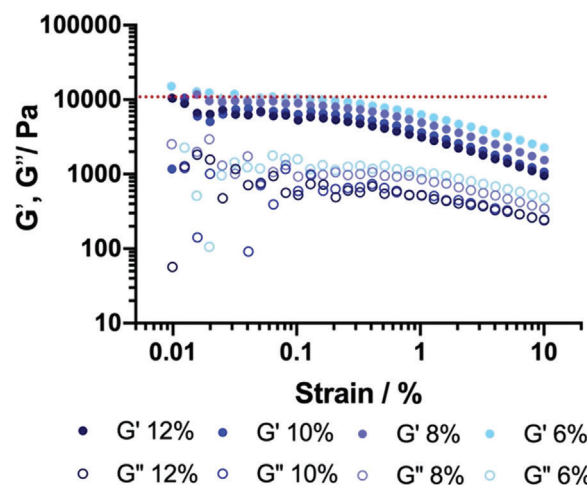


**Figure 7.** Oscillatory shear amplitude sweep measurements for mixtures of PEG-Ch (0.3% PEG equivalent in solution) with increasing amount of  $\alpha$ -CD. The horizontal line is added as the guide to the eye to identify the linear viscoelastic region (LVR).

12%  $\alpha$ -CD are shown in Figure 7. It was found that the LVR extends to  $\approx 0.2\%$  strain for all gels, a relatively narrow region that reflects quite fragile gels. While the LVR is rarely reported for hydrogels built from PEG/ $\alpha$ -CD inclusion complexes (IC), the observed brittleness of the gels is not surprising. The networks rely on hydrogen bonds between  $\alpha$ -CD threaded on adjacent (short) PEG chains, which induce the bundling and connection of the chains (or PPRs).<sup>[24]</sup> In other words, the gels are made of loosely connected particulates, whose solubility (and therefore capacity to hold water in their network) rely on the ability of the threaded  $\alpha$ -CD and PEG to also form hydrogen bonds with the solvent molecules; when these interactions are inhibited, phase separation occurs, as observed with some of the compositions studied (Figure 5). It has also been observed experimentally that this structure does lead to some solvent leaching out of the gels over time (syneresis).

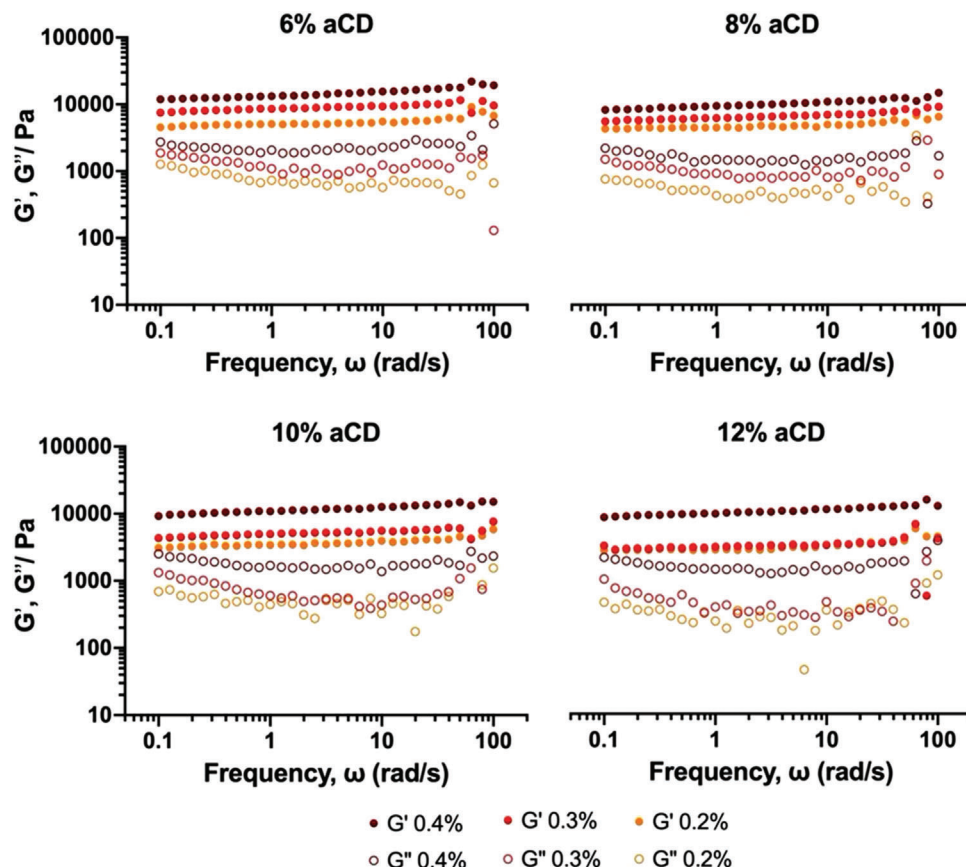


**Figure 8.** Effect of PEG-Ch on the rheology of the gels obtained from dynamic frequency sweep measurements for 6, 8, 10, and 12% of  $\alpha$ -CD with increasing PEG content: 0.2, 0.3, and 0.4% (displayed as averages between  $n = 4$  measurements).

Next, dynamic frequency sweep measurements were carried out to characterize the viscoelasticity of the gels. **Figure 8** presents the effect of PEG-Ch (expressed as the concentration of grafted PEG in solution) on hydrogels containing different concentrations of  $\alpha$ -CD: 6, 8, 10, and 12% w/w. The data show a remarkable independence of the elastic modulus ( $G'$ ) with frequency, and a slight dip in the viscous modulus  $G''$ . The data also suggest very long relaxation times for these materials, which can be estimated to be of the order of (or above)  $\approx 100$  s, as  $G'$  and  $G''$  do not cross within the range of frequencies measured. The elastic modulus ranges between  $\approx 3\,300$  and  $15\,500$  Pa for 12–6%  $\alpha$ -CD, taken at a frequency of  $10\text{ rad}\cdot\text{s}^{-1}$  (**Figure 9**), reflecting very stiff gels, for comparatively low concentrations of polymer (0.4–0.8% PEG-Ch). At all four  $\alpha$ -CD concentrations studied, increasing polymer concentration leads to increasing values of  $G'$  and  $G''$ . Regardless of  $\alpha$ -CD concentration, gels with the highest (0.4% PEG) and lowest (0.2% PEG) polymer content present the highest and lowest values of the elastic modulus, respectively. For a fixed polymer concentration, it is observed that decreasing  $\alpha$ -CD concentration leads to larger values of  $G'$  and  $G''$ , with the highest values obtained with 0.4% PEG-Ch. Based on the observation that gels could not be formed with 4%  $\alpha$ -CD, this highlights the fact that there is an optimum PEG/ $\alpha$ -CD ratio that achieves the highest elasticity. This means that beyond a threshold concentration, additional  $\alpha$ -CD molecules do not contribute to build addi-

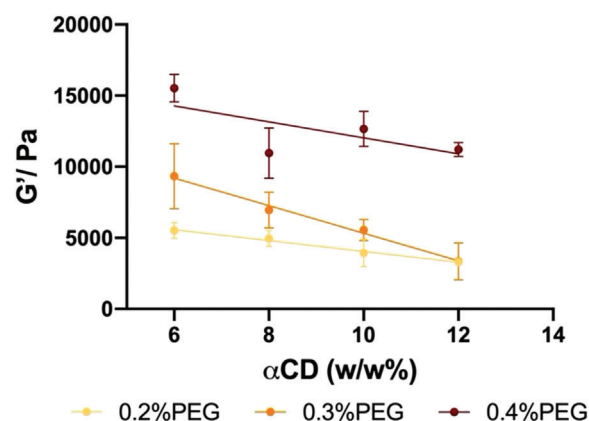


**Figure 9.** Effect of increasing  $\alpha$ -CD content for a range of PEG (0.2, 0.3, and 0.4% grafted PEG in solution, corresponding to 0.4, 0.6, and 0.8 PEG-Ch) on the elastic modulus ( $G'$ ) at a frequency of  $10\text{ rad}\cdot\text{s}^{-1}$ . Each point is an average between  $n = 4$  measurements.

tional elastically active junctions; they lead even, at very high  $\alpha$ -CD concentrations and low PEG-Ch (0.1%) to phase separation (**Figure 5**), as explained by the polymer coming out of solution due to extensive threading of the macrocycles on the chains and



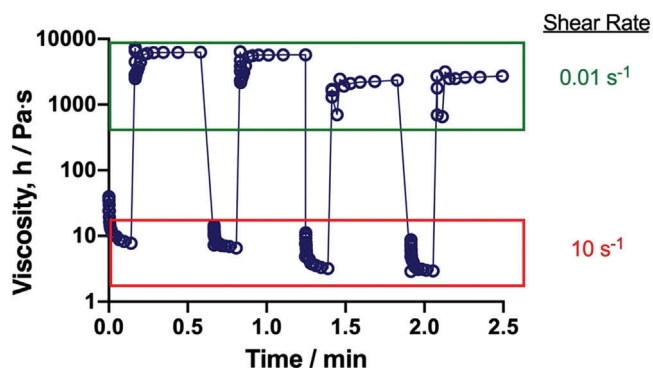


**Figure 10.** Shear-recovery viscosity curve for gels made of 0.3% PEG-Ch (expressed as grafted PEG content) with 10%  $\alpha$ -CD, performed over four cycles, alternating high shear rate ( $10 \text{ s}^{-1}$ , 10 s) and low ( $0.01 \text{ s}^{-1}$ , 30 s).

thus a reduction of hydrogen bonds between the polymer and water.

## 2.5. Rheology: Recoverability of the Gels After Stress

As these materials are built of weak, dynamic interactions, it is expected that these junctions can break and reform, making these gels suitable for application and recovery at the site of application. To assess their capacity to “heal” after strong shearing, steady-state shear measurements were conducted; this mimics the process of the gels recovering their structure and mechanical properties after the application of stress, experienced for instance by injection through a needle or spreading on the skin. Time-dependent viscosity curves were measured while alternating the shear rate from high ( $10 \text{ s}^{-1}$ ) to low ( $0.01 \text{ s}^{-1}$ ) for short periods of time (Figure 10). Due to the dynamic nature of the cross-links sustaining the networks, all gels present shear-thinning properties and a very low viscosity at high shear rate. Upon dropping the shear rate, gels recovered their high viscosity instantaneously, with values of  $\approx 6000 \text{ Pa}\cdot\text{s}$ . This thixotropic behavior was observed over the four consecutive cycles measured—with a small loss of viscosity ( $\approx 0.5\%$ ) from the third cycle, which was observed for all gel compositions studied (additional gel formulations are shown in Figure S1, Supporting Information).

## 3. Conclusion

This work reports the successful fabrication of supramolecular hydrogels based on chitosan grafted with polyethylene glycol moieties (5 kDa) and  $\alpha$ -cyclodextrin ( $\alpha$ -CD). These chitosan-based hydrogels are generated via the formation of polypseudorotaxanes (PPR) between  $\alpha$ -CD and PEG grafted on the chitosan backbones. The complexation and packing of these macrocycles along the PEG polymeric chains, and further interactions between  $\alpha$ -CD threaded on PEG attached to different chitosan chains, leads to the formation of microcrystalline domains, which act as junction points for a 3D network. XRD measurements confirmed the existence of the typical channel-like crystalline structures formed by the packing of the CDs, well-documented in PEG- $\alpha$ -CD gels and here present in these PEG-modified chitosan

gels. The generation of a hydrogel is dependent on the extent of grafting (it failed here with the lower degree of substitution of 11% but succeeded at 16%) and the ratio between polymer and  $\alpha$ -CD; specifically, gels were not formed with low amounts of CDs, while at low concentration of PEG, either weak gels were obtained (intermediate CD concentration) or phase separation occurred (high amount of CD), likely corresponding to a cross-linked polymer-rich phase and water. Oscillatory rheology measurements demonstrated a remarkable independence of the elastic modulus with frequency, suggesting very long relaxation times ( $>100 \text{ s}$ ) and remarkably stiff gels, with  $G'$  reaching values of  $\approx 15 \text{ kPa}$ , with moderate polymer concentrations (0.8%). Since the hydrogels are built on host-guest interactions, they are able to reform rapidly after being submitted to high stress, as demonstrated by steady-state rheological measurements where the shear was alternately set to a high and very low value, over several cycles, demonstrating their capacity to “heal.”

Overall, this simple strategy based on host-guest recognition and biocompatible molecules provides a way of generating useful materials with a remarkably high elastic modulus that can gel *in-situ* immediately after application to a topical or parenteral site, and thus have great potential for healthcare or cosmetic applications.

## 4. Experimental Section

**Materials:**  $\alpha$ -Cyclodextrin (98%) was purchased from Sigma-Aldrich (UK). Ultrapure water with a specific resistivity of  $18.2 \text{ M}\Omega\cdot\text{cm}$  was produced by a Purelab Ultra machine from ELGA Process Water (Marlow, UK).

Medium molecular-weight chitosan (190–310 kDa based on viscosity, 75–85% degree of deacetylation), trifluoroacetic acid (TFA),  $\text{D}_2\text{O}$ , methoxy-PEG-COOH (5 kDa), 1-ethyl-3-(3-dimethylaminopropyl)-carbodiimide hydrochloride (EDAC), and *N*-hydroxysuccinimide (NHS) were purchased from Sigma-Aldrich (Gillingham, UK). Sodium hydroxide was purchased from Fisher Scientific (UK). Dialysis membranes with a molecular cutoff 12–14 kDa were purchased from Medicell International Ltd., UK.

**Synthesis of PEGylated Chitosan (PEG-Ch):** PEGylated chitosan (PEG-Ch) was synthesized according to a published method with minor modifications.<sup>[40,45]</sup> LPEG-chitosan (LPEG-Ch, lower degree of PEGylation) was synthesized by initially dissolving chitosan (960 mg) in acetic acid (1% v/v, 138 mL). The mixture was continuously stirred for 20 h at room temperature. The pH of chitosan solution was increased to 6 using a 5 M NaOH solution. Then, PEG-COOH (702 mg) was added to the chitosan solution. After 15 min, NHS (81 mg) was added and stirred for 30 min. EDAC (134.4 mg) was then added and stirred for 24 h. The product was dialyzed against deionized water (4 L, eight total changes, 12–14 kDa) at room temperature for 3 days. The product was recovered by lyophilization using Heto Power Dry LL 3000 freeze-drier (Thermo Electron Corporation).

HPEG-chitosan (HPEG-Ch, higher degree of PEGylation) was synthesized, following the same procedure using 800 mg chitosan, 115 mL acetic acid, 1170 mg PEG-COOH, 135 mg NHS, and 224 mg EDAC. Note that HPEG-Ch is also referred to as PEG-Ch in the text, as it was studied more extensively due to its much higher solubility.

The % of yield was calculated according to Equation (1).

$$\text{Yield (\%)} = \frac{W_1}{W_2 + W_3} \times 100 \quad (1)$$

where  $W_1$ ,  $W_2$ , and  $W_3$  were the weights of the freeze-dried PEG-chitosan, weight of native chitosan, and PEG-COOH in the reaction mixture, respectively.

The percentage of grafting in weight (GW%) was calculated according to the method reported by Bhattarai et al.<sup>[46]</sup>

$$GW\% = \frac{W_t - W_c}{W_t} \times 100 \quad (2)$$

where  $W_t$  was the weight of the freeze-dried PEG-chitosan and  $W_c$  was the initial weight of chitosan used in the reaction mixture.

**Characterization of PEG-Ch:**  $^1\text{H}$  NMR spectra were recorded using a Bruker Nanobay 400 MHz NMR spectrometer. Unmodified chitosan (5 mg) was dissolved in acidified  $\text{D}_2\text{O}$  (1 mL  $\text{D}_2\text{O}$  with 10  $\mu\text{L}$  TFA). PEG-Ch (5 mg) was dissolved in 1 mL  $\text{D}_2\text{O}$ . The mixtures were stirred for 16 h at room temperature. The degree of substitution (DS) of PEG-Ch was calculated using  $^1\text{H}$  NMR spectroscopy by integrating a specific peak of PEG against specific chitosan peak in PEG-Ch using Equation 3:

$$DS\% = \frac{I(\text{OCH}_3)/3}{I(\text{H}_2)/1} \times 100 \quad (3)$$

FTIR spectra were recorded using a Spectrum 100 FTIR spectrophotometer (Perkin-Elmer, UK). The spectra were collected from an average of 16 scans, with a resolution of  $16\text{ cm}^{-1}$  over the range of  $4000\text{--}650\text{ cm}^{-1}$ .

**Aqueous Solubility of PEG-Chitosan (UV/Vis Spectroscopy):** Solubility of the unmodified chitosan and PEG-chitosan was measured at different pH values and fixed concentration at room temperature using a turbidimetric technique. The polymers were dissolved (0.05% w/w, 20 mL) in 1% v/v acetic acid and left stirring for 24 h. The turbidity (absorbance) of the systems was measured at room temperature using a BioTek Epoch plate reader at 400 nm using 1% v/v acetic acid as a blank. A total of 200  $\mu\text{L}$  aliquots were used. The pH was adjusted by the addition of either 1 M NaOH solution or 1% v/v acetic acid. The results are reported as the average of the turbidity of three samples at each pH point  $\pm$  standard deviation. Chitosan with the lower degree of PEGylation (LPEG-Ch) did not form gels with  $\alpha$ -CD and therefore was not analyzed further.

The aggregation and solubility of HPEG-Ch in water (natural pH) was assessed by turbidimetry using UV/Vis spectroscopy. HPEG-Ch solutions with increasing concentration (0.05–2% w/w) were prepared by mixing the freeze-dried product with water for 3 h (350 rpm) at  $22^\circ\text{C}$  and 1 h at  $75^\circ\text{C}$ . The mixtures were left to rest for 15 min, followed by sonication for 10 min using a water bath sonicator (281 FB11203, Fisher Scientific, UK). They were left to rest for 24 h and then centrifuged for 25 min at 6000 rpm before further use. The absorbance of the mixtures was recorded at 600 nm on a Lambda 2 spectrophotometer (Perkin Elmer, UK), at  $22^\circ\text{C}$ .

The absorbance was plotted as a function of HPEG-Ch concentration. When in solution, the turbidity from the samples was nearly zero and aggregation was detected by the linear increase of turbidity against concentration. The intersection of the two linear profiles was used as an estimation of the aggregation concentration.

**Preparation of Supramolecular Gels from HPEG-Ch and  $\alpha$ -CD:** Supramolecular gels were prepared by mixing a stock solution of HPEG-Ch (1.6% w/w) and either stock solutions (<12% w/w) or suspensions of  $\alpha$ -CD (up to 24% w/w) to achieve a range of compositions of HPEG-Ch (0.2–0.8% w/w) and  $\alpha$ -CD (2–12% w/w). The mixtures were left under mild stirring (350 rpm) for half an hour at room temperature and left to rest before further use (typically within a couple of days).

**Phase Diagrams:** HPEG-Ch solutions of 0.2–0.8% w/w concentration (corresponding to PEG content ranging between 0.1% and 0.4% w/w) were mixed with 2–12% w/w  $\alpha$ -CD solutions (0.04–0.2% mol). The solutions were mixed and stirred for 5 min at 350 rpm and the phase of the mixtures was assessed visually. The mixture was characterized as liquid, weak gel or gel (based on the observation of immediate flow, delayed flow, or no flow, respectively), and biphasic systems (where phase separation was observed). The phase diagram was built using R (version 3.6.0) and R studio (IDE version 1.1.463). The data were loaded and formatted using the package “readr” and the ternary graph was generated using the package “plotly.”

**Powder X-Ray Diffraction Measurements:** The freeze-dried samples were deposited on a glass holder and the X-ray diffractograms recorded

with a Bruker D8 Advance diffractometer, using the  $\text{Cu K}\alpha_1$  radiation ( $1.5406\text{ \AA}$ ), from  $5^\circ$  to  $40^\circ$  ( $2\theta$ ), with a step of  $0.02^\circ$  for a total time of 384 s (0.2 s per step).

**Rheological Measurements:** Oscillatory measurements were performed on an ARES strain-controlled rheometer (TA Instruments) fitted with a parallel plate geometry (8 mm diameter). Dynamic strain sweep tests (also known as amplitude sweeps, AS) were performed at a fixed frequency of  $6.28\text{ rad s}^{-1}$  to establish the linear viscoelastic region (LVR). Dynamic frequency sweep measurements (FS) were carried out in quadruplets with oscillation frequencies within the range  $0.1\text{--}100\text{ rad s}^{-1}$  and a fixed strain of 0.1% (within the LVR). Finally, steady-state measurements were performed in triplicates to assess the recovery of the gels after shearing, by alternating short periods of high shear rate ( $10\text{ s}^{-1}$ ) and very low shear rate ( $0.01\text{ s}^{-1}$ ). All rheological measurements were done at  $20 \pm 0.1^\circ\text{C}$  (controlled by a Peltier unit).

## Supporting Information

Supporting Information is available from the Wiley Online Library or from the author.

## Acknowledgements

Erasmus the wonderful EU program to support education, training, youth and sport in Europe is acknowledged for funding the three-month internship of C.P. at the Institute of Pharmaceutical Science, visiting from ENSIC (Université de Lorraine, France).

## Conflict of Interest

The authors declare no conflict of interest.

## Data Availability Statement

The data that support the findings of this study are available from the corresponding author upon reasonable request.

## Keywords

chitosan, cyclodextrins, host-guest, hydrogels, polypseudorotaxane

Received: November 11, 2022

Revised: January 4, 2023

Published online:

- [1] C. A. Dreiss, *Curr. Opin. Colloid Interface Sci.* **2020**, *48*, 1.
- [2] S. J. Buwalda, K. W. M. Boere, P. J. Dijkstra, J. Feijen, T. Vermonden, W. E. Hennink, *J. Control. Rel.* **2014**, *190*, 254.
- [3] J. Li, X. J. Loh, *Adv. Drug. Deliv. Rev.* **2008**, *60*, 1000.
- [4] X. Liu, X. Chen, M. X. Chua, Z. Li, X. J. Loh, Y. L. Wu, *Adv. Healthcare Mater.* **2017**, *6*, 1700159.
- [5] C. Xu, Y. L. Wu, Z. Li, X. J. Loh, *Mater. Chem. Front.* **2019**, *3*, 181.
- [6] A. Singh, J. Zhan, Z. Ye, J. H. Elisseeff, *Adv. Funct. Mater.* **2013**, *23*, 575.
- [7] N. Liu, J. Chen, J. Zhuang, P. Zhu, *Int. J. Biol. Macromol.* **2018**, *117*, 553.
- [8] P. K. Sharma, M. Halder, U. Srivastava, Y. Singh, *ACS Appl. Bio. Mater.* **2019**, *2*, 5313.

- [9] E. Lih, J. S. Lee, K. M. Park, K. D. Park, *Acta Biomater.* **2012**, *8*, 3261.
- [10] K. Saekhor, W. Udomsinprasert, S. Honsawek, W. Tachaboonyakiat, *Int. J. Biol. Macromol.* **2019**, *123*, 167.
- [11] J. Yu, W. Ha, J. N. Sun, Y. P. Shi, *ACS Appl. Mater. Interfaces* **2014**, *6*, 22.
- [12] Y. Niu, T. Guo, X. Yuan, Y. Zhao, L. Ren, *Soft Matter* **2018**, *14*, 1227.
- [13] J. Li, X. Li, X. Ni, X. Wang, H. Li, K. W. Leong, *Biomaterials* **2006**, *27*, 4132.
- [14] B. Schmidt, C. Barner-Kowollik, *Angew. Chem., Int. Ed.* **2017**, *56*, 8350.
- [15] B. W. Liu, H. Zhou, S. T. Zhou, J. Y. Yuan, *Eur. Polym. J.* **2015**, *65*, 63.
- [16] J. Szejtli, Introduction and General Overview of Cyclodextrin Chemistry | Chemical Reviews [Internet]. [cited 2 September 2020]. <https://pubs.acs.org/doi/10.1021/cr970022c>
- [17] T. Loftsson, M. Másson, M. E. Brewster, *J. Pharm. Sci.* **2004**, *93*, 1091.
- [18] M. E. Davis, M. E. Brewster, *Nat. Rev. Drug Discov.* **2004**, *3*, 1023.
- [19] K. K. A. Vandra, P. Picconi, M. Valero, G. González-Gaitano, A. Woods, N. M. M. Zain, K. D. Bruce, L. A. Clifton, M. W. A. Skoda, K. M. Rahman, R. D. Harvey, C. A. Dreiss, *Mol. Pharm.* **2020**, *17*, 2354.
- [20] Y. Li, J. Li, X. Zhao, Q. Yan, Y. Gao, J. Hao, J. Hu, Y. Ju, *Chemistry* **2016**, *22*, 18435.
- [21] F. van de Manakker, T. Vermonden, C. F. van Nostrum, W. E. Hennink, *Biomacromolecules* **2009**, *10*, 3157.
- [22] C. B. Rodell, A. L. Kaminski, J. A. Burdick, *Biomacromolecules* **2013**, *14*, 4125.
- [23] C. Loebel, C. B. Rodell, M. H. Chen, J. A. Burdick, *Nat. Protoc.* **2017**, *12*, 1521.
- [24] M. Ceccato, P. Lo Nostro, P. Baglioni, *Langmuir* **1997**, *13*, 2436.
- [25] J. Li, A. Harada, M. Kamachi, *Polym. J.* **1994**, *26*, 8.
- [26] E. Sabadini, T. Cosgrove, W. Taweeprada, *Langmuir* **2003**, *19*, 4812.
- [27] C. A. Dreiss, T. Cosgrove, F. N. Newby, E. Sabadini, *Langmuir* **2004**, *20*, 9124.
- [28] K. L. Liu, Z. Zhang, J. Li, *Soft Matter* **2011**, *7*, 11290.
- [29] K. M. Huh, T. Ooya, W. K. Lee, S. Sasaki, I. C. Kwon, S. Y. Jeong, N. Yui, *Macromolecules* **2001**, *34*, 8657.
- [30] M. A. da Silva, C. A. Dreiss, *Polym. Int.* **2016**, *65*, 268.
- [31] M. Serres-Gómez, G. González-Gaitano, D. B. Kaldybekov, E. D. H. Mansfield, V. V. Khutoryanskiy, J. R. Isasi, C. A. Dreiss, *Langmuir* **2018**, *34*, 10591.
- [32] L. Casettari, D. Vllasaliu, E. Castagnino, S. Stolnik, S. Howdle, L. Illum, *Prog. Polym. Sci.* **2012**, *37*, 659.
- [33] Y. I. Jeong, D. G. Kim, M. K. Jang, J. W. Nah, *Carbohydr. Res.* **2008**, *343*, 282.
- [34] N. N. Porfiryeva, R. I. Moustafine, V. V. Khutoryanskiy, *Polym. Sci. Ser. C* **2020**, *62*, 62.
- [35] E. V. R. Campos, J. L. Oliveira, L. F. Fraceto, *Front. Chem.* **2017**, *5*, 1.
- [36] W. M. Facchinatto, A. Fiamingo, D. M. dos Santos, S. P. Campana-Filho, *Int. J. Biol. Macromol.* **2019**, *124*, 828.
- [37] K. M. Huh, Y. W. Cho, H. Chung, I. C. Kwon, S. Y. Jeong, T. Ooya, W. K. Lee, S. Sasaki, N. Yui, *Macromol. Biosci.* **2004**, *4*, 92.
- [38] L. Casettari, D. Vllasaliu, G. Mantovani, S. M. Howdle, S. Stolnik, L. Illum, *Biomacromolecules* **2010**, *11*, 2854.
- [39] M. M. T. Ways, S. K. Filippov, S. Maji, M. Glassner, M. Ceglowski, R. Hoogeboom, S. King, W. M. Lau, V. V. Khutoryanskiy, *J. Coll. Interface Sci.* **2022**, *626*, 251.
- [40] Q. Luo, H. Gao, L. Peng, G. Liu, Z. Zhang, *J. Appl. Polym. Sci.* **2016**, *133*, 43465.
- [41] M. Sugimoto, M. Morimoto, H. Sashiwa, H. Saimoto, Y. Shigemasa, *Carbohydr. Polym.* **1998**, *36*, 49.
- [42] J. Du, Y. L. Hsieh, *Cellulose* **2007**, *14*, 543.
- [43] S. Mao, X. Shuai, F. Unger, M. Wittmar, X. Xie, T. Kissel, *Biomaterials* **2005**, *26*, 6343.
- [44] I. N. Topchieva, A. E. Tonelli, I. G. Panova, E. V. Matuchina, F. A. Kalashnikov, V. I. Gerasimov, C. C. Rusa, M. Rusa, M. A. Hunt, *Langmuir* **2004**, *20*, 9036.
- [45] C. Prego, M. Fabre, D. Torres, M. J. Alonso, *Pharm. Res.* **2006**, *23*, 549.
- [46] N. Bhattarai, H. R. Ramay, J. Gunn, F. A. Matsen, M. Zhang, *J. Control. Rel.* **2005**, *103*, 609.